COMPARISON OF MODAL ANALYSIS METHODS APPLIED TO A VIBRO-ACOUSTIC TEST ARTICLE

Jocelyn Pritchard
Research Engineer
Structural Dynamics Branch
NASA Langley Research Center
Hampton, VA 23681

Ralph Buehrle
Senior Research Engineer
Structural Acoustics Branch
NASA Langley Research Center
Hampton, VA 23681

Richard Pappa
Senior Research Engineer
Structural Dynamics Branch
NASA Langley Research Center
Hampton, VA 23681

Ferdinand Grosveld
Aerospace Engineering Manager
Lockheed Martin
NASA Langley Research Center
Hampton, VA 23681

ABSTRACT

Modal testing of a vibro-acoustic test article referred to as the Aluminum Testbed Cylinder (ATC) has provided frequency response data for the development of validated numerical models of complex structures for interior noise prediction and control. The ATC is an all aluminum, ring and stringer stiffened cylinder, 12 feet in length and 4 feet in diameter. The cylinder was designed to represent typical aircraft construction. Modal tests were conducted for several different configurations of the cylinder assembly under ambient and pressurized conditions. The purpose of this paper is to present results from dynamic testing of different ATC configurations using two modal analysis software methods: Eigensystem Realization Algorithm (ERA) and MTS IDEAS Polyreference method. The paper compares results from the two analysis methods as well as the results from various test configurations. The effects of pressurization on the modal characteristics are discussed.

INTRODUCTION

Design optimization and noise control applications in the aerospace and transportation industries require accurate structural vibration and acoustic response predictions. Recent work at NASA Langley Research Center [1-7] has examined the development and validation of finite element modeling techniques for aircraft structures to better predict the dynamic response. The Aluminum Testbed Cylinder (ATC) was designed and fabricated using aircraft construction techniques to provide a generic structure for experimental validation of numerical modeling techniques and optimization methods for the prediction and control of aircraft interior noise. The first series of experiments were modal tests to validate and update the finite element model of the ATC. This paper describes the ATC hardware, modal testing procedure, and experimental modal analysis results. In particular, modal analysis results obtained using the Eigensystem Realization Algorithm (ERA) [8] and MTS IDEAS Polyreference [9] method are compared for several different test configurations. The test configurations correspond to various levels of assembly of the ATC and culminate with the fully assembled ATC under pressurized conditions.

1 TEST SETUP AND PROCEDURE

1.1 Description of ATC Configurations

The Aluminum Testbed Cylinder (ATC) was fabricated to resemble typical aircraft fuselage construction. Figures 1 and 2 show the primary components of the ATC. The cylindrical section of the ATC is an all-aluminum structure that is 12 feet in length and 4 feet in diameter. The shell consists of a 0.040-inch skin stiffened by 11 ring frames and 24 equally spaced longitudinal stringers. Double lines of rivets and epoxy attach the skin to the frames and stringers. Two-inch thick particleboard end plates provide stiff, terminating reflective surfaces for the enclosed acoustic cavity. The end domes are ¼-inch thick fiberglass composite structures allowing for pressurization of the interior to 7 psi to simulate flight conditions at altitudes up to 35000 feet. The end plates contain several ½-inch diameter holes to allow the pressure on each side of the end plates to equalize during pressurized tests.

Table 1 lists the configurations that were tested. Configurations I, II, and III were tested and discussed in a previous paper[2]. Configurations IV, V, and VI have recently been tested and the results are discussed in this paper. Configuration VII is planned for future work.

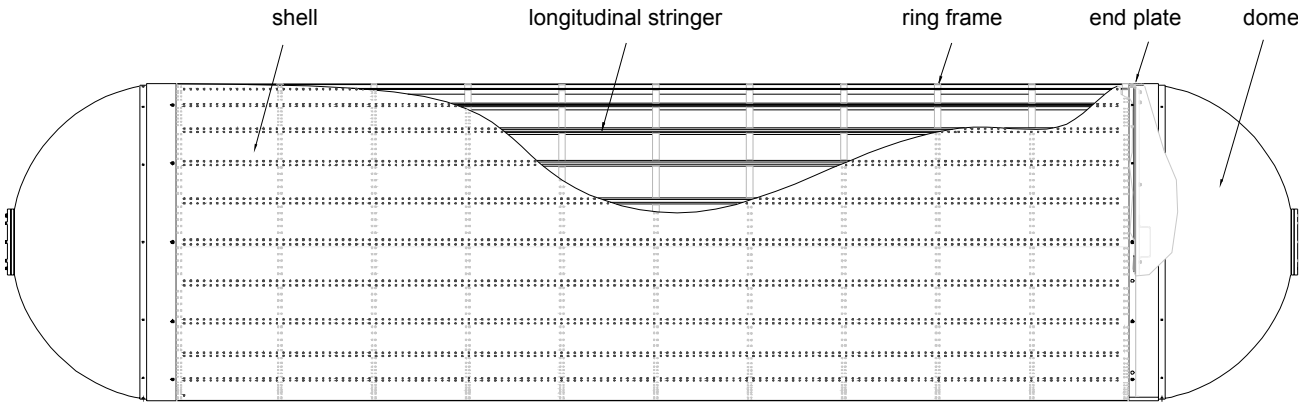

Figure 1: Aluminum Testbed Cylinder (ATC) primary components.

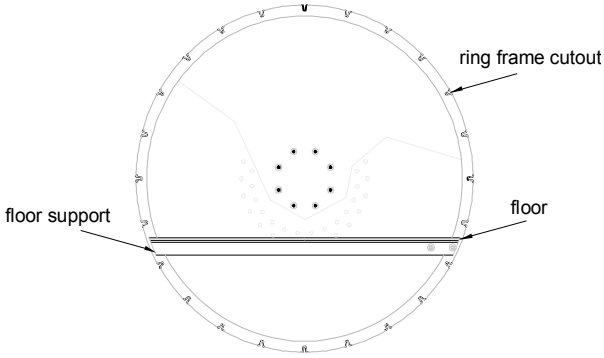

Figure 2: End view of ATC showing ring frame, honeycomb floor, and floor support.

Configuration I consists of the bare ring and stringer frame. The two particle board endplates are attached to the frame in Configuration II. Each endplate weighs approximately 100 lbs. Configuration III is the bare frame (Configuration 1) covered with the aluminum skin. Configuration IV has the endplates attached as well as the aluminum skin. Configuration V has a dome on each end of the cylinder to allow an internal pressure of up to 7 psi. Each of the end dome components weighs about 80 lb. They are designed to safely carry the loads from the internal pressure without applying unwanted bending loads to the cylinder. The floor is constructed of aluminum honeycomb and is supported by cross members at each of the ring frames. The floor is situated 9 inches below the centerline of the cylinder. Testing of this cylinder configuration has been postponed to a later date. The fully assembled cylinder weighs approximately 600 lbs and is shown in Figure 3a.

Table 1: Test configurations and status for Aluminum Testbed Cylinder (ATC)

Conf. #	*Description*	*Status*
I	Bare Frame	Complete
II	Conf. I + endplates	Complete
III	Conf. I + skin	Complete
IV	Conf. III + endplates	Complete
V	Conf. IV + domes (Fig 3)	Complete
VI	Conf. V + pressure	Complete
VII	Conf. VI + floor	Future

1.2 Description of Test Apparatus and Setup

Figure 3b shows the overall setup for the modal tests on the fully assembled ATC. The ATC is supported on four airbag isolators to simulate free-free boundary conditions. Four shakers were used simultaneously for all tests. The placement of the sensors and shakers was predetermined based on pre-test predictions of the first 100 modes. Figure 4 is a photograph of the test setup showing a close-up of shaker 3 and 4 in the background. Shakers 1 and 2 are located on the opposite side of the cylinder. Shaker 1 applied a tangential side force at a 45 degree angle below horizontal which primarily excites torsional and axial modes of the structure. Shakers 2, 3, and 4 apply radial excitation in order to excite the bending and shell modes of the structure. Most of the accelerometers (see figure 4) are positioned in the radial direction (normal to the cylinder surface) since this is the direction of most interest for acoustic interior noise prediction. There are also biaxial sensor measurements including tangential to the surface and at the end rings there are triaxial measurements taken

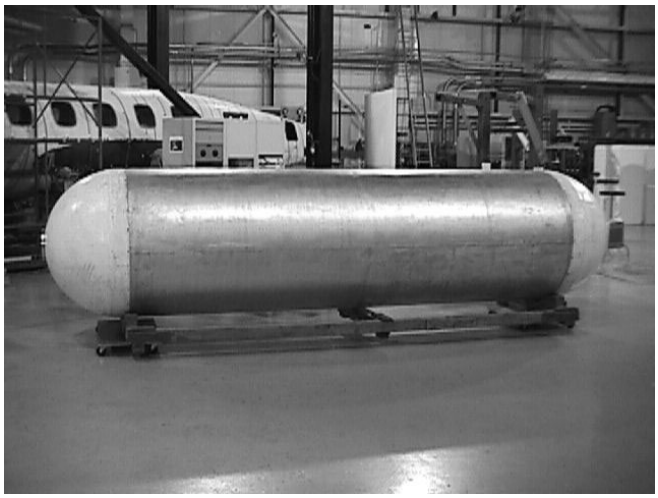

Figure 3a: The Aluminum Testbed Cylinder (ATC) fully assembled.

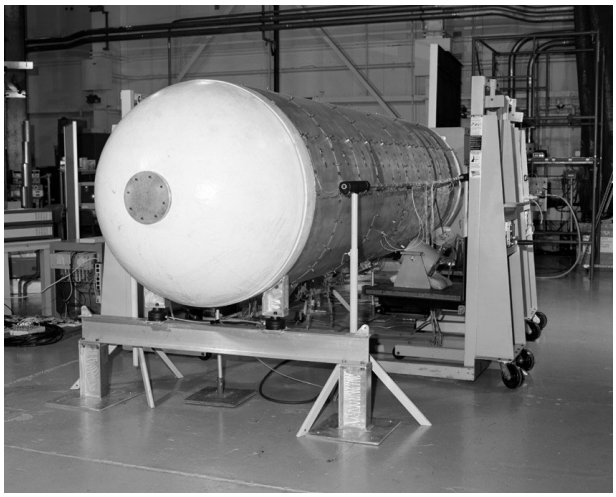

Figure 3b: The Aluminum Testbed Cylinder instrumented for testing.

including the longitudinal direction (along the length of the cylinder).

1.3 Test Procedures

A Zonic data acquisition system (DAS) was used to record 228 response measurements and 4 excitation inputs. Computer controlled signal conditioning was used to optimize the voltage amplitudes and low pass (LP) noise filters were used on each channel to filter out high frequency instrumentation noise. The force and acceleration time histories were recorded on several analog-to-digital converter (ADC) throughput disks in the Zonic DAS where anti-aliasing and autoranging capabilities ensure high quality measurements. Modal tests used all four shakers simultaneously with continuous random signals. Data was collected in each modal test for 16.3 minutes. The frequency response functions had 12,800 frequency lines from 0 to 1000 Hz, resulting in a frequency resolution of 0.078125 Hz. They were generated using 75 ensemble averages.

1.4 Numerical Analysis

Experimental modal analyses of the ATC have generated frequency response data for Configurations I through VI. The modal results are being used to validate and refine finite element models of these configurations. The correlation between experimental results and the modal data from the initial finite element analyses for Configuration III are discussed in References 1 and 5. Refinements of these finite element models have included

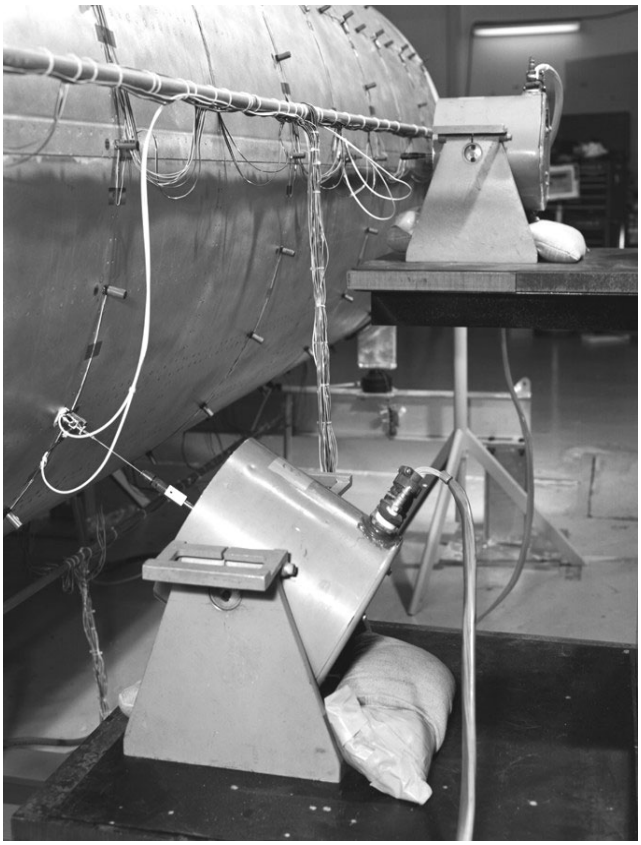

Figure 4: Photograph of test setup showing a close-up of shaker 3.

optimized use of the ring frame quadrilateral and beam elements and the detailed modeling of the riveted ring frame/longitudinal stiffener junctions. Table 2 lists the first fifteen experimental and analytical modal frequencies for

the refined ATC baseline cylinder (Configuration III). These modes are flexible modes and no rigid body modes were included. Radial-axial modes are described by the parameters i and j where i is the number of circumferential waves in the mode shapes and j is the number of axial or longitudinal half waves in the mode shapes. Good agreement (less than 9 percent difference) was obtained between the predicted and measured modal frequencies of the refined finite element model. Detailed results and discussion on the development and validation of the numerical models for all configurations will be reported in future publications.

Table 2: First fifteen experimental and numerical modal frequencies of the ATC baseline cylinder (Configuration III)

Analysis Frequency [Hz]	Modal Test Frequency [Hz]	Mode Description	Analysis /Test Difference [%]
53.073	50.820	i=2, j=0 (1)	4.43
53.073	51.176	i=2, j=0 (2)	3.71
56.723	53.462	i=2, j=0 (1)	6.10
56.723	54.287	i=2, j=0 (2)	4.48
108.04	100.146	i=2, j=1 mode (1)	7.88
108.04	102.123	i=2, j=1 mode (2)	5.79
142.86	141.375	i=3, j=1 mode (1)	1.05
142.86	142.348	i=3, j=1 mode (2)	0.36
158.10	152.390	i=3, j=2 mode (1)	3.74
158.10	152.411	i=3, j=2 mode (2)	3.75
169.16	160.102	i=3, j=3 mode (1)	5.66
169.16	161.829	i=3, j=3 mode (2)	4.53
193.22	183.553	i=3, j=4 mode (1)	5.26
193.22		i=3, j=4 mode (2)	
222.19	204.342	i=2, j=2 mode (1)	8.73

2. ANALYSIS METHODS USED FOR DATA REDUCTION

2.1 Eigensystem Realization Algorithm (ERA)

ERA[8] is a multiple-input, multiple-output, time domain technique that uses all available frequency response functions simultaneously to identify structural modal parameters. The method was developed at NASA Langley Research Center in 1984 and has been continuously improved upon since then as it has been used in many applications. A brief explanation of the ERA data analysis procedure is given next.

The experimental frequency response functions are converted into impulse response functions by inverse Fourier transformation. Two generalized Hankel matrices are constructed H(0) and H(1) using the impulse response data. Generally, the size of a Hankel matrix is dependent on the number of modes in the frequency range of interest and the number of measurement points. The number of modes that are assumed in the analysis has an effect on the accuracy of the modal parameters. With ideal, noise-free data having N modes, there are exactly 2N non-zero singular values. An nth order ERA state-space realization is performed from which modal damping rates are found.

ERA is composed of subroutines to perform the various steps in the data analysis procedure, such as filtering, calculating mode indicator functions (mifs), plotting, generating Hankel matrices, decomposition, state space realization, and animation of modes. A mode condensation process automatically finds the optimum number of assumed modes to be used in the calculation of the modal parameters for each frequency based on the mode confidence factors. This process essentially takes the guesswork out of deciding the number of modes to include for insuring a good estimate of the modal parameters. This seems to allow the user to analyze a wider range of frequencies at one time.

2.2 Polyreference (IDEAS)

The Polyreference Method[9] is a time domain curve fitting approach that uses impulse response functions acquired from inverse Fourier transformation of the frequency response functions (similar to ERA). This method uses frequency response data from multiple references in a global least squares fashion. A correlation matrix is constructed using frequency response functions from selected reference locations. The generation of this matrix is dependent on the choice of references since this determines the weighting of the poles in the accumulation of the matrix. From this matrix the resonant frequencies and damping values (poles) are estimated. Finally, the residue for each pole at every response location is estimated and the mode shape is extracted from this information. The frequency-domain polyreference method was used for mode shape estimation for the results included in this paper.

IDEAS has a user interface that leads the user through the pertinent steps in the data analysis process. Additionally, the software stores and manages all function data sets that may be readily accessed through a task menu or button display panel within the user interface. To achieve good curve fits it was advantageous to divide the data into several frequency ranges. The number of poles needed for inclusion in the analysis for optimum parameter estimation

is typically not known and the number is not the same for all frequencies.

3. RESULTS

Radial-axial modes are described by parameters i and j where i is the number of circumferential waves in the mode shape and j is the number of axial or longitudinal half waves in the mode shape. Except for the axial and torsion modes, the modes occur in pairs at approximately the same frequency due to the symmetric nature of the cylinder.

3.1 Comparison of Results from ERA and IDEAS Polyreference Data Analysis Methods

Figures 5-7 show plots of the correlation of all ERA-identified modes with all IDEAS-identified modes using the modal assurance criterion (MAC) for ATC configurations IV, V, and VI respectively. The MAC is the square of the inner product of normalized mode shape vectors. A value of 80% or more indicates a high degree of similarity between the modes.[10] Each row and column in the plots represent one mode. The size of the rectangle that is located at the intersection of two modes is proportional to the MAC value. For example, if the MAC value is 88% then the rectangle covers 88% of the height and width of the intersecting area. For MAC values above 80% the rectangles are filled. The three plots shown give the correlation results from three test cases: Configuration IV, V, and VI with 6psi of internal pressure. (Note that Configuration V and VI with 0 psi internal pressure are equivalent.)

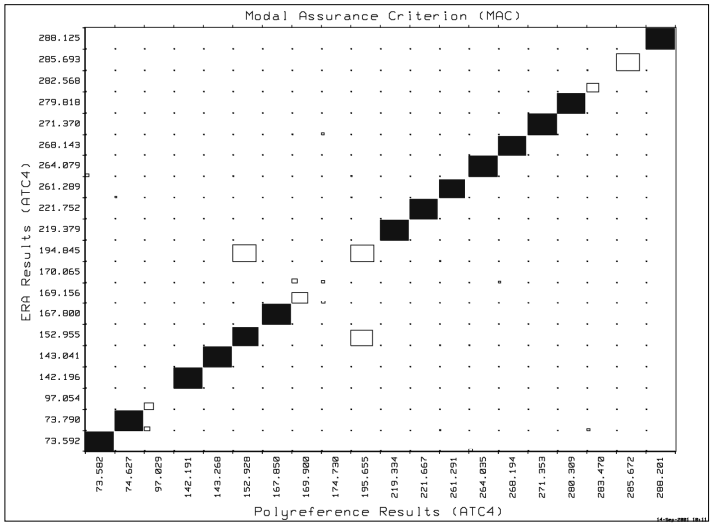

Figure 5: Correlation of ERA and IDEAS mode shapes for configuration IV using MAC

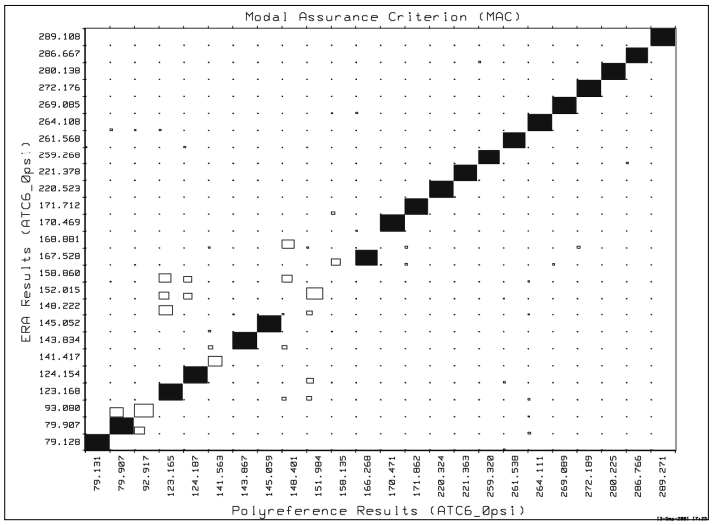

Figure 6: Correlation of ERA and IDEAS mode shapes for configuration V using MAC.

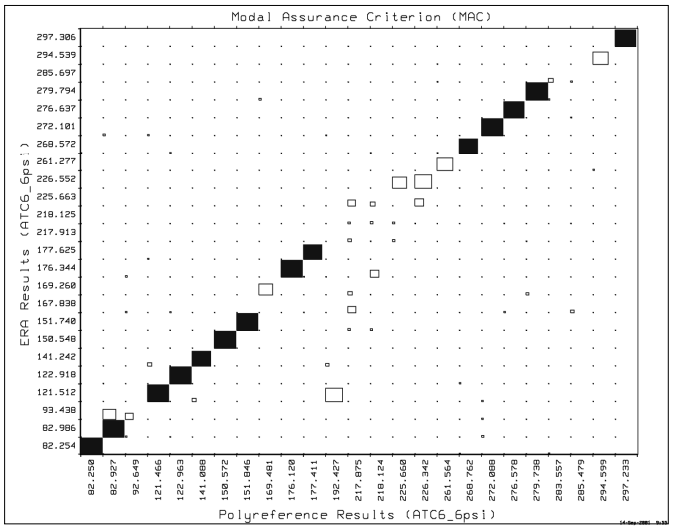

Figure 7: Correlation of ERA and IDEAS mode shapes for ATC configuration VI using MAC.

As indicated by the filled rectangles along the diagonal of each of the three plots, the correlation between the ERA analyses and the IDEAS Polyreference method is very good. Except for an approximate mid range of modes on each of the three plots, most of the MAC values are 80% or higher. The third mode on all three plots exhibits off-diagonal squares indicating a difference between the two analyses. This mode for Configuration VI with 6 psi internal pressure (93 Hz) is compared for both analytical methods in figure 8a and b. The mode appears to be an axial mode (along the length of the cylinder, z direction).

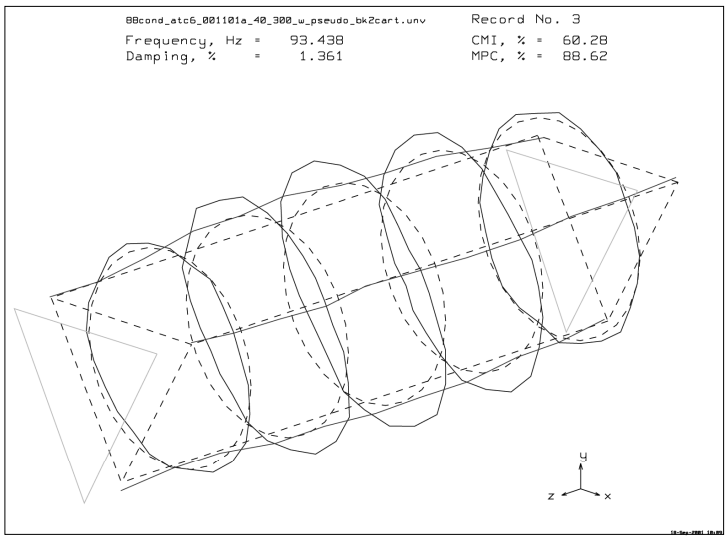

Figure 8a: Mode shape generated from ERA.

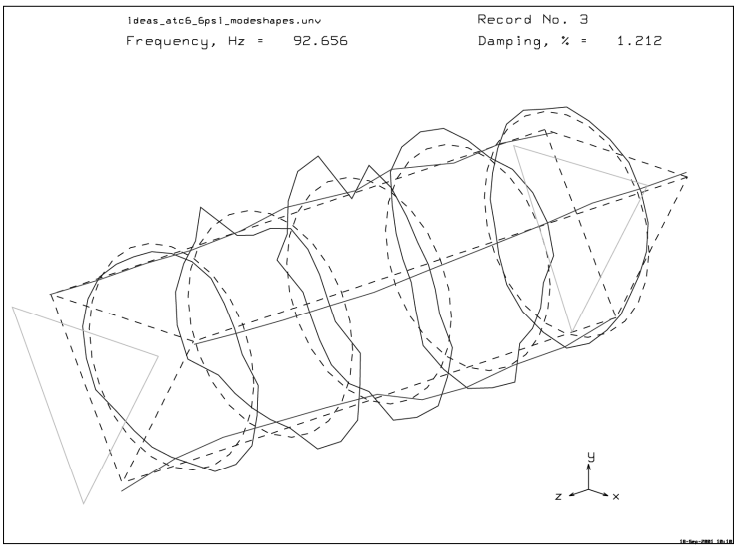

Figure 8b: Mode shape generated from IDEAS.

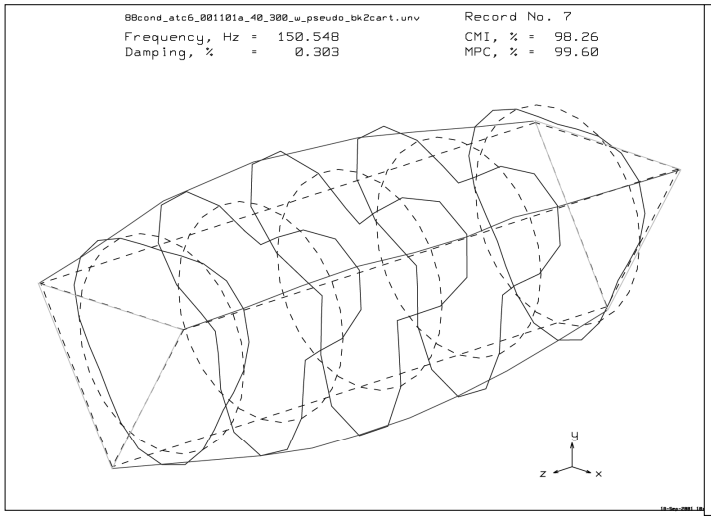

Figure 9a: Mode shape generated from ERA.

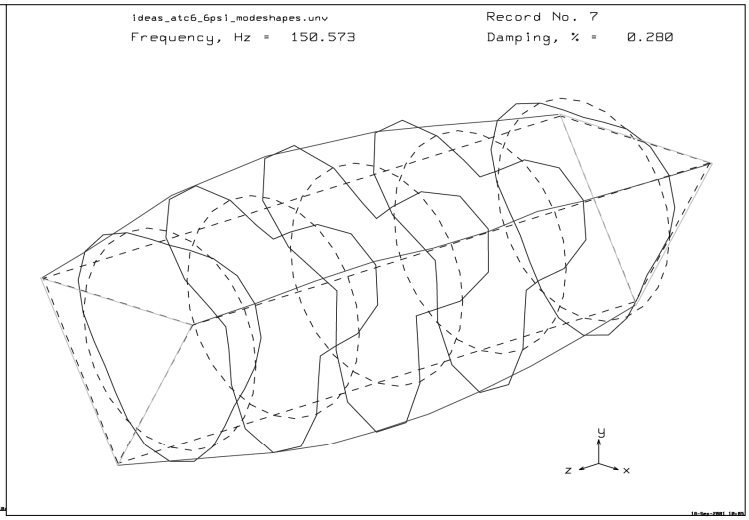

Figure 9b: Mode shape generated from IDEAS.

However, since there are only a limited number of accelerometers (located only at the end rings) measuring motion in the axial direction it is difficult to capture the mode characteristics. The mode may have computational errors or have residual effects from nearby modes. Some discrepancies are evident between the two mode estimates when the correlation is not good.

Examination of figure 7 for this configuration shows the IDEAS Polyreference method found a frequency at 192 Hz that was not found with the ERA analysis. The identification of this mode shape was not very clear. Conversely, a mode (i=2, j=2) was identified in ERA at 167.8 Hz that was not found by IDEAS. This was also true in figure 6 for Configuration V. Interestingly this mode (170 Hz from ERA and 174 Hz from IDEAS) was identified in both analysis methods in Configuration IV but correlation was poor (see figure 5). Figure 9 shows an example of mode shapes where the two analysis methods correlated very well. This is the radial-axial mode with i=3, j=1 at 150

Hz for Configuration VI with 6 psi internal pressure. The mode shapes appear to be identical. This mode correlated well in all three configurations.

3.2 Comparison of Results from Configurations IV and V

Table 3 contains a list of the identified modes from both analysis methods from 0 to 300 Hz for Configuration IV. Similarly, table 4 contains a list of identified modes from 0 to 300 Hz for Configuration V. In comparing the results in Tables 3 and 4, the higher order frequencies (above 220 Hz) of radial-axial modes do not vary drastically between configuration IV and V where the difference in configuration is the addition of end domes in configuration V. In general the frequencies from Configuration V are similar to the same modes on Configuration IV. Configuration V introduces a torsion mode at 141 Hz and distinct X and Y bending modes at 123.2 Hz and 124.2 Hz (first X and Y bending modes) that are not seen in Configuration IV.

3.3 Effects of Pressurization

Comparison of results from configuration V and VI with 6 psi internal pressure shows the effects of pressurization of the cylinder on modal parameters. Table 5 contains a list of the identified modes from 0 to 300 Hz from both analysis methods for Configuration VI with 6 psi internal pressure. In comparing tables 4 and 5, the frequencies of the 6 psi (Configuration VI) case are significantly higher than those in the 0 psi (Configuration V) case except for the bending and torsion modes which are slightly less than the 0 psi configuration. A bending mode was identified at 192 Hz in configuration VI (6 psi) with the IDEAS analysis that is similar to the mode identified by both analyses at 152 Hz for configuration V (0 psi). There is not enough evidence to conclude that this mode was significantly increased in frequency between the unpressurized and pressurized configurations.

Table 3: Identified modes from Configuration IV

ATC IV Frequency, Hz		Description
Polyreference	ERA	
73.6	73.6	l=2, j=1
74.6	73.8	l=2,j=1
97.0	97.1	Axial
142.2	142.2	l=3, j=1
143.3	143.0	l=3, j=1
152.9	153.0	First bending
167.9	167.8	l=3, j=2
169.9	169.2	l=3, j=2
174.7	170.1	l=2, j=2
195.7	194.8	XY-Bending?
219.3	219.4	l=3, j=3
221.7	221.8	l=3,j=3
261.3	261.3	l=4, j=1
264.0	264.0	l=4, j=1
268.2	268.1	l=4, j=2
271.4	271.4	l=4, j=2
280.3	279.8	l=3, j=4

Table 4:Identified modes from Configuration V

ATC V (0 psi) Frequency, Hz		**Description**
Polyreference	**ERA**	
79.1	79.1	l=2, j=1
79.9	79.9	l=2, j=1
92.9	93.1	Axial
123.2	123.2	First X bending
124.2	124.2	First Y bending
141.6	141.4	First torsion
143.9	143.8	l=3, j=1
145.1	145.1	l=3, j=1
148.4	148.2	
152.0	152.0	XY-bending?
158.1	158.9	
166.3	167.5	l=2, j=2
	168.9	l=2, j=2
170.5	170.5	l=3, j=2
171.9	171.7	l=3, j=2
220.3	220.5	l=3, j=3
221.4	221.4	l=3, j=3
259.3	259.3	l=2, j=3
261.5	261.6	l=4, j=1
264.1	264.1	l=4, j=1
269.1	269.1	l=4, j=2
272.2	272.2	l=4, j=2
280.3	280.1	l=3, j=4
286.8	286.7	I=4, j=3
289.3	289.1	I=4, j=3

Table 5: Identified modes from Configuration VI with 6 psi internal pressure.

ATC VI (6 psi)	Frequency, Hz	Description
Polyreference	**ERA**	
82.3	82.3	l=2, j=1
82.9	83.0	l=2, j=1
92.7	93.4	Axial
121.5	121.5	First X-bending
123.0	122.9	First Y-bending
141.1	141.2	First torsion
150.6	150.5	l=3, j=1
151.8	151.7	l=3, j=1
	167.8	l=2, j=2
169.5	169.3	l=2, j=2
176.1	176.3	l=3, j=2
177.4	177.6	l=3, j=2
192.4		XY-bending?
217.9	217.9	l=3, j=2
218.1	218.1	l=3, j=2
225.7	225.7	l=3, j=3
226.4	226.6	l=3, j=3
261.6	261.3	?
268.8	268.6	l=4, j=1
272.1	272.1	l=4, j=1
276.6	276.6	l=4, j=2
279.7	279.8	l=4, j=2
283.6		l=3, j=4
285.5	285.7	l=3, j=4
294.6	294.5	l=4, j=3
297.2	297.3	l=4, j=3

CONCLUSIONS

Modal testing of a vibro-acoustic test article referred to as the Aluminum Testbed Cylinder (ATC) was conducted for several different assembly configurations under ambient and pressurized conditions. The data analysis was performed using two modal analysis software methods: Eigensystem Realization Algorithm (ERA) and MTS IDEAS Polyreference method. The paper compared results from the two analysis methods as well as the results from various test configurations.

The modal test activities on the ATC have resulted in a large database of frequency response functions and modal parameter estimates corresponding to the various levels of assembly. This database is being used to validate and update finite element models of the ATC. The comparison of results from the Eigensystem Realization Algorithm (ERA) and the IDEAS Polyreference analysis methods was very good with the exception of a few hard-to-determine modes. These discrepancies may be due to the experimental setup pertaining to the number or placement of the sensors on the structure as opposed to any inadequacies of either analysis method.

REFERENCES

[1] **Buehrle, R. D., Fleming, G. A., Pappa, R. S., and Grosveld, F. W**., "Finite Element Model Development for Aircraft Fuselage Structures", Sound and Vibration Magazine, January 2001, Acoustical Publications, Inc.

[2] **Pappa, R. S., Pritchard, J. I., and Buehrle, R. D**., "Vibro-Acoustics Modal Testing at NASA Langley Research Center," NASA/TM-1999-209319, May 1999.

[3] **Grosveld, F. W**., "Structural Normal Mode Analysis of the Aluminum Testbed Cylinder", AIAA Paper 98-1949, Proceedings of the 39th AIAA/ASME/ASCE Structures, Structural Dynamics, and Materials Conference, Long Beach, CA, April 1998.

[4] **Fleming, G. A., Buehrle, R. D., and Storaasli, O. L.**, "Modal Analysis of an Aircraft Fuselage Panel Using Experimental and Finite Element Techniques", Proceedings of the 3rd International Conference on Vibration Measurements by Laser Techniques, Ancona, Italy, June 1998.

[5] **Buehrle, R. D., Fleming, G. A., Pappa, R. S., and Grosveld, F. W.,** "Finite Element Model Development and Validation for Aircraft Fuselage Structures", Proceedings of the 18th International Modal Analysis Conference, San Antonio, Texas, February 7-10, 2000.

[6] **Buehrle, Ralph D., Robinson, Jay H. and Grosveld, Ferdinand W.,** "Vibro-Acoustic Model Validation for a Curved Honeycomb Composite Panel", AIAA Paper 2001-1587, presented at the 42nd AIAA/ASME/ASCE/AHS/ASC Structures, Structural Dynamics, and Materials Conference, Seattle, WA, 16-19 April 2001.

[7] **Grosveld, Ferdinand W., Buehrle, Ralph D. and Robinson, Jay H.,** "Numerical and Acoustic Modeling of a Curved Composite Honeycomb Panel", AIAA Paper 2001-2277, presented at the 7th AIAA/CEAS Aeroacoustics Conference, Maastricht, The Netherlands, 28-30 May, 2001.

[8] **Pappa, R. S., Schenk, A., Niedbal, N., and Klusowski, E.,** "Comparison of Two Dissimilar Modal

Identification Techniques", Journal of Guidance, Control, and Dynamics, Vol. 15, No. 4, pp.840-846, July-August 1992.

[9] **Crowley, J. R., Rocklin, G. T., Hunt, D. L., and Vold, H.,** "The Practical Use of the Polyreference Modal Parameter Estimation Method", Proceedings of the 3rd International Modal Analysis Conference, Schenectady, N.Y., January 28-31, 1985.

[10] **Pappa, R. S.,** "Independent Analysis of the Space Station Node Modal Test Data", Journal of Guidance, Control, and Dynamics, Vol.22, No. 1, pp. 22-27, January-February, 1999.